



Effect of high-intensity ultrasound on the physicochemical properties, microstructure, and stability of soy protein isolate-pectin emulsion

Tong Wang^a, Ning Wang^a, Na Li^a, Xiaorui Ji^a, Hongwei Zhang^{a,*}, Dianyu Yu^{a,*}, Liqi Wang^b

^a School of Food Science, Northeast Agricultural University, Harbin 150030, China

^b School of Computer and Information Engineering, Harbin University of Commerce, Harbin 150028, China

ARTICLE INFO

Keywords:

High-intensity ultrasound
Emulsion
Stability
Soy protein isolate
Pectin

ABSTRACT

In this study, an emulsion stabilized by soy protein isolate (SPI)-pectin (PC) complexes was prepared to investigate the effects of high-intensity ultrasound (HIU) treatment (150–600 W) on the physicochemical properties, microstructure, and stability of emulsions. The results found that the emulsion treated at 450 W showed the best emulsion stability index (ESI) (25.18 ± 1.24 min), the lowest particle size (559.82 ± 3.17 nm), the largest ζ -potential absolute value (16.39 ± 0.18 mV), and the highest adsorbed protein content (27.31%). Confocal laser scanning microscopy (CLSM) and atomic force microscopy (AFM) revealed that the emulsion aggregation was significantly improved by ultrasound treatment, and the average roughness value (Rq) was the smallest (10.3 nm) at 450 W. Additionally, HIU treatment reduced the interfacial tension and apparent viscosity of the emulsion. Thermal stability was best when the emulsion was treated at 450 W, D_{43} was minimal (907.95 ± 31.72 nm), and emulsion separation also improved. Consequently, the creaming index (CI) was significantly decreased compared to the untreated sample, indicating that the storage stability of the emulsion was enhanced.

1. Introduction

Soy protein isolate (SPI) is a high-quality and inexpensive plant protein. Due to its amphiphilic characteristics, it can absorb at the oil–water interface, and is often used as an emulsifier in the food industry [1,2]. However, SPI is affected by processing conditions such as pH [3], resulting in protein aggregation and precipitation. The addition of stabilizers can improve the stability of protein emulsions, and studies have proved that polysaccharides are the preferred stabilizers [4,5]. Pectin (PC) is a natural anionic polysaccharide in plant cell walls [6]. Due to its wide availability and low price, it is a commonly used additive in the food industry and has excellent properties such as gelling and thickening [7]. Therefore, protein and polysaccharide complexation studies have received great attention recently to improve emulsion performance [8].

In emulsions stabilized by protein-polysaccharide complexes, proteins and polysaccharides are complexed through hydrogen bonding, van der Waals forces, electrostatic and hydrophobic interactions [9–11], and wrapped on the surface of oil droplets, which effectively prevents droplet aggregation and improves emulsion stability. Xu et al. [12] used soybean polysaccharides and sodium caseinate to stabilize emulsions,

forming a dense interfacial membrane through electrostatic attraction and hydrophobic interactions, thus promoting emulsion stability. Taherian et al. [13] obtained a whey protein isolate and fish gelatin complex through layer-by-layer interfacial deposition, and found that the complex emulsion had better physical and chemical stability than an emulsion stabilized by protein alone.

High-intensity ultrasound (HIU) treatment can promote emulsification. Different from commonly used methods of reducing emulsion particle size through high shear and high pressure, HIU treatment emulsifies through its unique cavitation effect. The cavitation effect and physical force generated by ultrasound directly affect the oil droplets and liquid in the emulsion. Then, the droplets are broken into small particles to obtain the emulsion with smaller particle size [14]. Concurrently, the large amount of energy generated by the cavitation effect will also cause chemical, physical, and thermal effects on the substances in the emulsion [15]. Therefore, under the above effects, the emulsion properties will be affected by the treatment [16]. Taha et al. [17] explored the effect of different ultrasound conditions on the characteristics of SPI-stabilized emulsions containing medium chain triglycerides. They found that the treated emulsion had better emulsion stability and a higher amount of interfacial proteins. Liu et al. [18]

* Corresponding authors.

E-mail addresses: zhanghongwei@neau.edu.cn (H. Zhang), dyyu2000@126.com (D. Yu).

<https://doi.org/10.1016/j.ultsonch.2021.105871>

Received 8 November 2021; Received in revised form 6 December 2021; Accepted 9 December 2021

Available online 10 December 2021

1350-4177/© 2021 The Authors.

Published by Elsevier B.V. This is an open access article under the CC BY-NC-ND license

(<http://creativecommons.org/licenses/by-nc-nd/4.0/>).

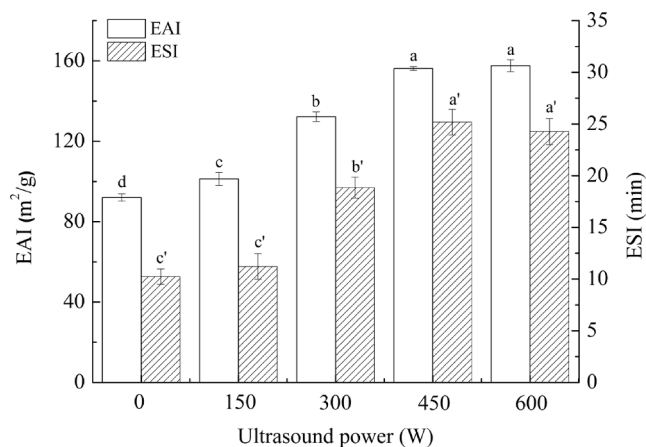


Fig. 1. Emulsifying properties analysis under different ultrasound powers Note: The superscript letters in the same group indicate significant differences among the data ($p < 0.05$).

Table 1

Changes of mean particle size (D_{43}), PDI and ζ -potential of emulsion treated by high intensity ultrasound under different powers.

Ultrasound power (W)	D_{43} (nm)	PDI	ζ -potential
0	1706.00 \pm 6.46 ^a	0.801 \pm 0.098 ^a	-8.55 \pm 0.32 ^a
150	1142.20 \pm 4.66 ^b	0.349 \pm 0.039 ^{bc}	-11.47 \pm 0.25 ^b
300	834.87 \pm 5.78 ^c	0.263 \pm 0.064 ^c	-13.11 \pm 0.47 ^c
450	559.82 \pm 3.17 ^e	0.265 \pm 0.045 ^c	-16.39 \pm 0.18 ^e
600	638.80 \pm 6.53 ^d	0.433 \pm 0.072 ^b	-15.71 \pm 0.22 ^d

Note: The different superscript letters in the same column indicate significant differences between the data ($p < 0.05$).

evaluated the effect of different HIU powers on the stability of myofibrillar protein (MP) emulsions, and found that the MP emulsion stability was significantly improved at 450 W.

Herein, based on the advantages of HIU technology, such as high energy, low price, convenient operation, environmental friendliness, and high safety, an SPI-PC complex emulsion was prepared by HIU treatment. The effects of different HIU powers on the physicochemical

properties, microstructure, and stability of emulsion were investigated, and the mechanism of the HIU effect on SPI-PC emulsions was explored to solve the problem of large particle size and unstable combination, enhance the emulsification characteristics of the complex, and increase the stability of the emulsification system, which provided emulsifiers with low price and good functional properties for the food industry.

2. Materials and methods

2.1. Materials

SPI was self-made in the laboratory. Defatted soybean powder was mixed with deionized water and the pH was adjusted to 8.0. The dispersion was subjected to protein extraction with magnetic stirring for 2.5 h and then centrifuged at $10000 \times g$ and 4°C for 30 min. The pH of the supernatant was adjusted to 4.5 and centrifuged at $10000 \times g$ for 30 min. The precipitate was washed twice with deionized water, and then

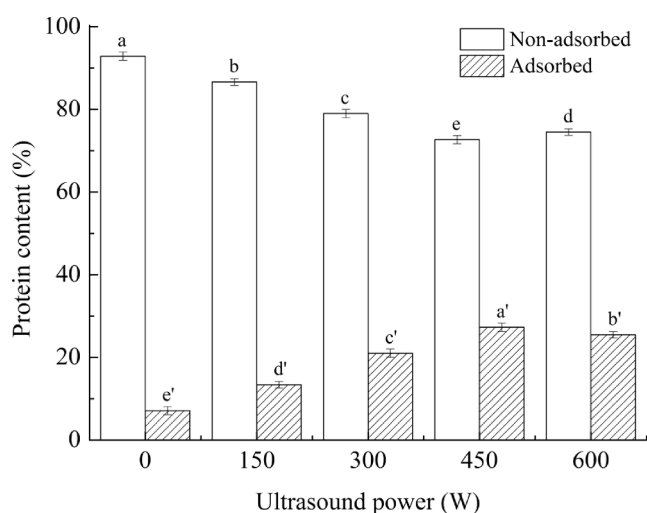


Fig. 3. Interfacial proteins distribution under different ultrasound powers Note: The superscript letters in the same group indicate significant differences among the data ($p < 0.05$).

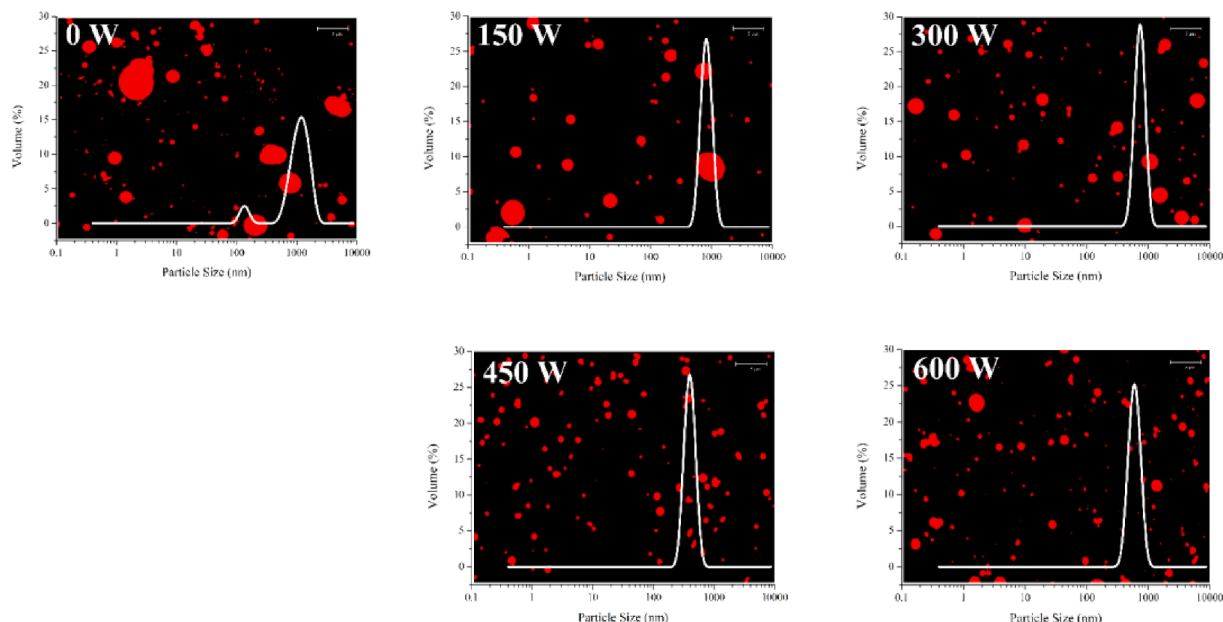


Fig. 2. CLSM and particle distribution under different ultrasound powers.

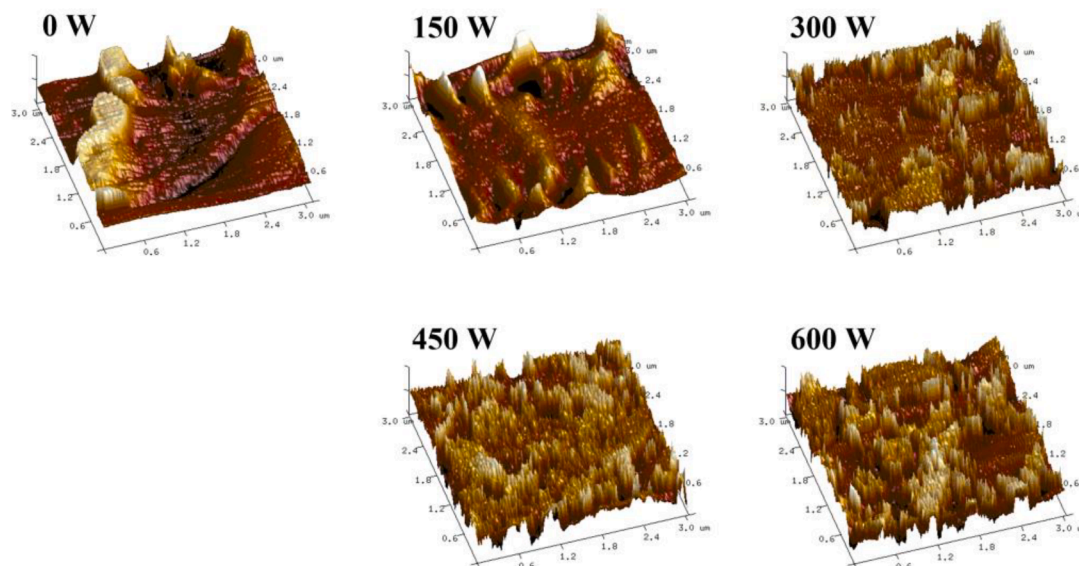


Fig. 4. AFM analysis under different ultrasound powers.

neutralized to pH 7.0. The neutral solution was frozen and subsequently freeze-dried for further use. The protein content of the SPI was determined to be $90.34 \pm 0.91\%$ by the Kjeldahl method. High methoxy methyl ester pectin was obtained from Yuanye Bio-technology Co., Ltd (Shanghai, China). First grade soybean oil was purchased from Yihai Kerry (Harbin) Oils, Grains & Foodstuffs Industries Co., Ltd (Harbin, China).

2.2. Preparation of complex

SPI and PC were dissolved in phosphate buffer solution (pH 7.0, 0.01 M), respectively. After stirring, the SPI and PC solutions were mixed, and the SPI and PC mass fractions in the final solution were 1% and 0.3%, respectively. Then, citric acid was added to the solution to adjust the pH to 3.5 and stirred. Consequently, 0.01% NaN_3 was added to the solution and stored at 4°C overnight to obtain SPI-PC complexes.

2.3. Preparation of emulsion

The SPI-PC mixed solution was taken, and 10% (v/v) soybean oil was added. The emulsion stabilized by the SPI-PC complex was prepared with a homogenizer (Ultra-Turrax T18, Angni Co., Shanghai, China) at 20000 rpm for 5 min. Then, the freshly prepared emulsion was ice-bathed to maintain the temperature below 20°C , and the emulsion was subjected to 150, 300, 450, and 600 W HIU treatment for 15 min by using a Scientz-II D ultrasound generator (Scientz Biotechnology Co., Ltd., Ningbo, China). Ultrasonic conditions: frequency 20 kHz, pulse working time 4 s, intermittent time 2 s, and an ultrasonic titanium probe with a diameter of 6 mm was immersed into the emulsion at a depth of 1 cm from the bottom. Consequently, the emulsions were stored at 4°C until further analysis.

2.4. Determination of emulsifying properties

Emulsifying properties were measured by the method of Li et al. [19] with some modifications. Briefly, 0.1% (w/v) sodium dodecyl sulfate was diluted 100-fold and added to 50 μL of fresh emulsion. The absorbance of the diluted emulsion at 500 nm was measured with a spectrophotometer. The emulsion activity index (EAI) and emulsion stability index (ESI) were calculated as follows:

$$\text{EAI}(\text{m}^2/\text{g}) = \frac{2 \times 2.303 \times A_0 \times \text{DF}}{10000 \times \theta \times L \times C}$$

$$\text{ESI}(\text{min}) = \frac{A_0 \times 10}{A_0 - A_{10}}$$

Here, A_0 is the absorbance at 0 min, DF is the dilution factor (100), C is the protein concentration (g/mL) before emulsification, θ is the oil volume fraction (v/v) of the emulsion, L is the optical path (1 cm), and A_{10} is the absorbance at 10 min.

2.5. Determination of particle size and ζ -potential

The particle size of the emulsions treated with different ultrasound powers was measured by a Mastersizer 2000 particle size analyzer (Malvern Instrument Co., Ltd., UK.). The volume mean diameter (D_{43}) was used to describe the particle size of the samples. Moreover, the ζ -potential of the emulsions was measured.

2.6. Confocal laser scanning microscopy (CLSM)

The distribution of the emulsions under different ultrasound powers was evaluated according to the method of Geremias-Andrade et al. [20]. First, Nile red was dissolved in isopropanol to obtain a 0.1% dyeing solution. Subsequently, 20 μL Nile Red was added to 0.5 mL of emulsions and stained for 30 min. Then, the stained emulsions were placed on concave microscope slides and covered with glycerol-coated coverslips to obtain confocal images.

2.7. Distribution of interfacial proteins

Emulsions were centrifuged at $10000 \times g$ for 30 min to separate the non-adsorbed and adsorbed proteins as reported by Jiang et al. [21]. Afterward, the cream phase was removed, and the serum phase was collected using a long needle syringe and filtered through a 0.45 μm filter. The amounts of non-adsorbed and adsorbed proteins present in the serum and cream phase were calculated using Lowry's method.

2.8. Atomic force microscopy (AFM)

The micromorphology of the emulsions under different ultrasound powers was observed by AFM. The emulsions were placed on a freshly cleaved mica sheet and then air dried at room temperature. The images and average roughness value (R_q) of the emulsions were analyzed by Nanoscope Software.

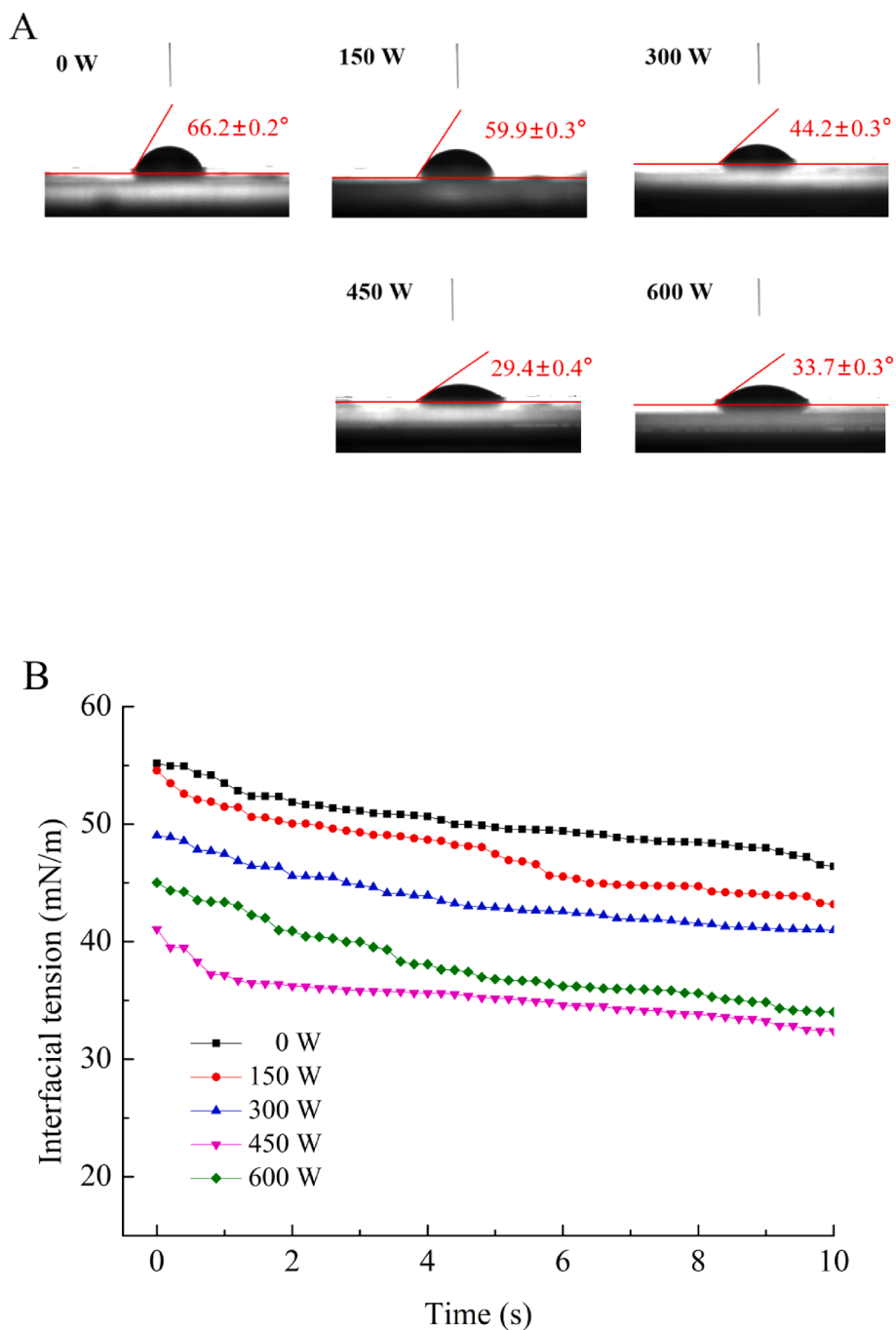


Fig. 5. Contact angle and interfacial tension analysis under different ultrasound powers.

2.9. Contact angle

The contact angle of the emulsions was determined by the sessile drop method. Briefly, a small amount of emulsion was smeared on a glass slide to form a film with a diameter of approximately 10 mm. A high-precision syringe was used to put a drop of water on the surface of the film formed by the emulsion, and then the image of the drop was recorded immediately after falling from the syringe. The contour of the drop was numerically solved and fitted to the Laplace-Young equation to determine the interfacial tension.

2.10. Apparent viscosity

Static rheological measurements of the emulsions under different

ultrasound powers were recorded using a rheometer. The shear rate was increased from 0.1 s^{-1} to 1000 s^{-1} . The relationship between the shear rate and the apparent viscosity was recorded and analyzed.

2.11. Thermal stability

The emulsions treated with different ultrasound powers were heated in a boiling water bath with a temperature of $100 \text{ }^\circ\text{C}$ for 20 min, then cooled to room temperature. After standing for 30 min, the particle size distribution was evaluated by a particle size analyzer.

2.12. Storage stability

The freshly prepared emulsions were stored at $25 \text{ }^\circ\text{C}$ for 30 days. The

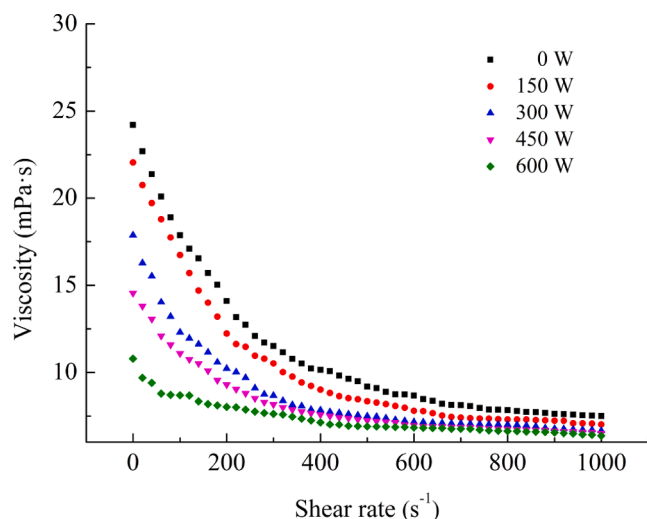


Fig. 6. Apparent viscosity analysis under different ultrasound powers.

creaming index (CI) was obtained by determining the height of the clear liquid (Hc) and the total height of the emulsion (Ht), and the calculation equation can be expressed as follows:

$$CI(\%) = \frac{Hc}{Ht} \times 100$$

2.13. Statistical analysis

All data were obtained in triplicate. The standard error was analyzed and the data were recorded by Origin 9.1. Statistics 22.0 was used to analyze variance, and Duncan's test ($p < 0.05$) was utilized to evaluate the significance of differences in the data.

3. Results and discussion

3.1. Emulsifying properties analysis

Emulsifying properties reflect the ability of emulsifiers to form and stabilize emulsions by adsorbing to the oil–water interface and reducing the interfacial tension [22]. Fig. 1 exhibits the emulsifying properties of SPI-PC complexes stabilized emulsions treated by HIU at different powers. Compared with the untreated emulsion, the EAI and ESI of the HIU-treated emulsions increased with increasing HIU powers from 0 to 450 W. The emulsion treated at 450 W had the best emulsifying properties, and the EAI and ESI increased by 69.69% and 145.66%, respectively. Wang et al. [23] found that HIU treatment could effectively reduce the particle size of the complex and improve the dispersion and solubility of the complex. In addition to modifying proteins and polysaccharides, HIU usually generates powerful micro jets to make the emulsion system more uniform. However, the emulsifying properties did not continue to increase when the emulsion was treated at 600 W ($p > 0.05$). This may be because excessive HIU power may destroy the spherical structure of SPI and form large aggregates, resulting in reduced emulsifying properties [24].

3.2. Particle size, PDI, and ζ -potential analysis

The D_{43} , PDI, and ζ -potential values of the emulsions treated at different powers are exhibited in Table 1. The D_{43} and PDI of the emulsions decreased with increasing HIU power. When the emulsion was treated at 450 W, the D_{43} of the emulsion was the smallest. During the ultrasound treatment, the energy generated by cavitation caused the complexes and droplets to be violently agitated resulting in a reduction of the particle size. When the HIU power was 600 W, the D_{43} and PDI of

the emulsion increased again. This may account for the aggregation of the complex. The role of ultrasound in particle size reduction has been widely demonstrated [25]. Wang et al. [26] showed that the shear force and turbulence generated by cavitation could cause protein dispersion, and the particle size of complexes significantly reduced. The decrease in particle size allowed more complexes to be adsorbed on the oil–water interface, which was beneficial to improve emulsion stability. ζ -potential can characterize the degree of electrostatic attraction or repulsion between adjacent particles in an emulsion system, and it is also a key indicator of emulsion stability. Compared with the untreated emulsion, the absolute value of the ζ -potential increased significantly after HIU treatment, and reached the maximum at 450 W. The increase in the absolute value of the ζ -potential would enhance the electrostatic repulsion between protein and inhibit aggregation, thereby promoting emulsion stability [27]. This was also one of the reasons for the improved emulsifying properties.

3.3. CLSM and particle distribution

Fig. 2 presents the CLSM micrographs and particle size distribution of the emulsions. The untreated emulsion had a large particle size and uneven distribution, and local aggregation occurred. With increasing HIU treatment power, the emulsion aggregation was significantly improved. When the treatment power reached 450 W, the particle size of the emulsion was the smallest, which was consistent with the results in Section 3.2. This was attributed to the physical force caused by ultrasound, which resulted in the emulsion droplets being effectively broken, thus the particle size decreased. Zhu et al. [28] reported that the emulsifying properties of walnut protein were improved by ultrasound treatment, which may be due to the formation of smaller droplets and the higher surface hydrophobicity of the ultrasound-treated protein particles.

3.4. Distribution of interfacial proteins

The interfacial protein distribution will affect the stability of the emulsion interface layer, which is closely related to the stability of the emulsion [29]. The change in protein content at the emulsion interface under different HIU treatments is shown in Fig. 3. As the HIU power increased from 0 W to 450 W, the adsorbed protein content in the emulsion gradually increased from 7.12% to 27.31%, and the non-adsorbed protein content decreased from 92.88% to 72.69%. The increase in adsorbed protein content might be due to the cavitation caused by ultrasound treatment, which reduced the droplet size, and increased the surface area of the droplets [30]. Concurrently, HIU treatment induced the changes in the spatial arrangement of protein molecules, and proteins with smaller particle diameters were spread to the surface of the oil droplets faster, which increased the content of the adsorbed protein. Therefore, the interfacial protein content increased during emulsion formation, and the emulsion stability was improved. When the HIU power reached 600 W, the adsorbed protein content in the emulsion was slightly reduced, and the non-adsorbed protein content increased. This phenomenon indicated that high-power treatment might cause the protein to form aggregates, reduce the content of adsorbed protein on the surface of the oil droplets, and increase the droplet size, which was not conducive to the formation of stable and uniform emulsions. The results were consistency with the results of particle size and ζ -potential.

3.5. AFM analysis

AFM was used to study the microstructure and surface morphology of the emulsions treated by HIU at different powers. In Fig. 4, the untreated emulsion showed significant aggregation. As the HIU power increased, the aggregation phenomenon was alleviated. When the emulsion was treated at 450 W, the peaks in the AFM image were more uniform, demonstrating that the formed emulsion was evenly dispersed

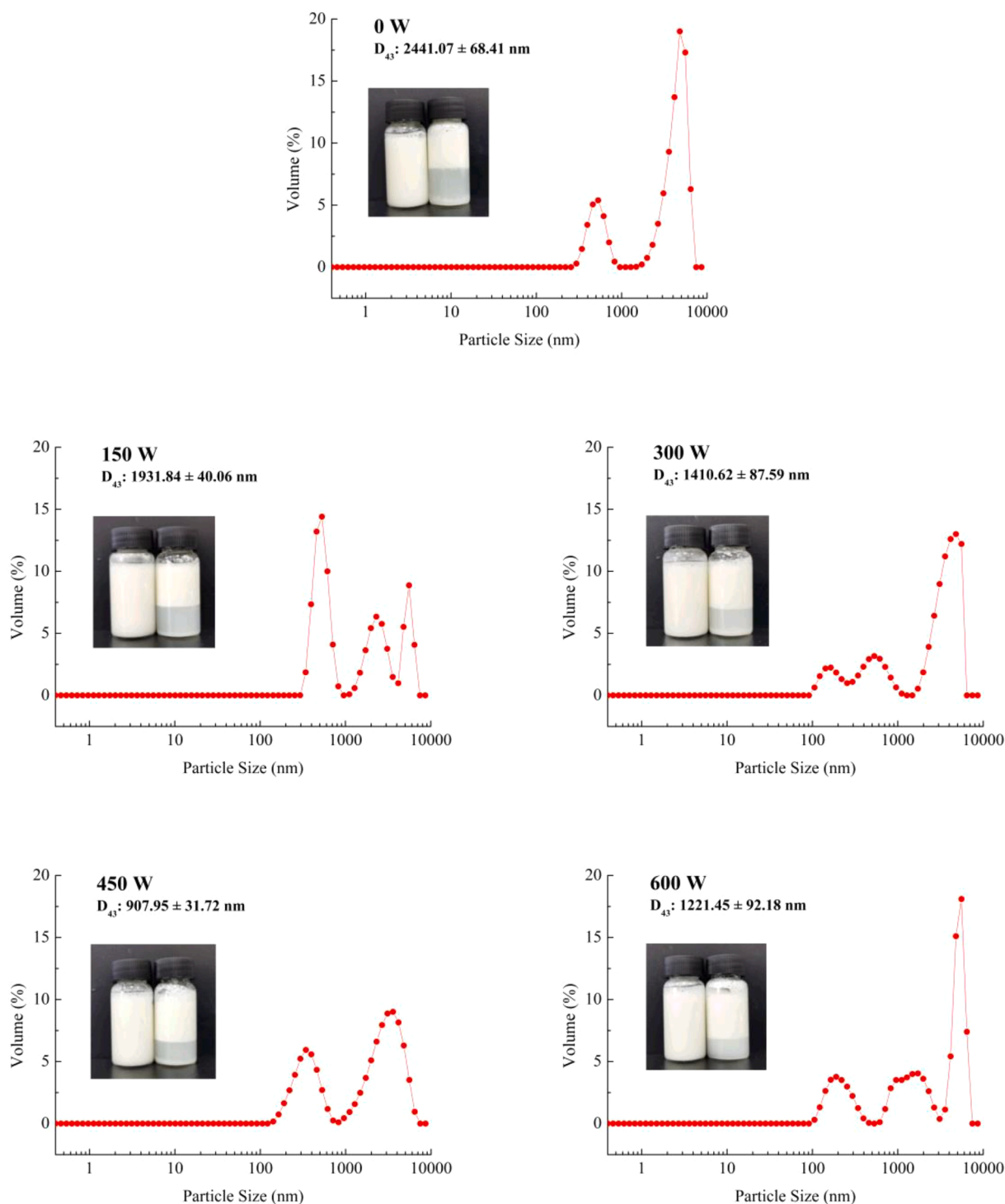


Fig. 7. Thermal stability analysis under different ultrasound powers.

with small particles and had good stability, which was consistent with the CLSM results. Besides, Rq, as an indicator of surface roughness, can reflect the degree of aggregation. The Rq of the untreated emulsion was the largest (38.5 nm). In contrast, the Rq of the emulsion after ultrasound treatment decreased significantly ($p < 0.05$). The minimum Rq (10.3 nm) at 450 W suggested that the emulsion had the best dispersibility. Nevertheless, when the emulsion was treated at 600 W, the Rq increased to 14.6 nm, and the AFM image showed a tendency to aggregate, which may be related to the formation of insoluble aggregates [31]. Xiong et al. [32] found the similar phenomenon that

excessive ultrasound caused changes in the molecular structure of proteins and reduced their emulsifying properties. Therefore, an appropriate HIU treatment power can significantly improve emulsion aggregation.

3.6. Contact angle and interfacial tension analysis

The contact angle (θ) is an important indicator to evaluate the wettability of emulsions. When $\theta < 90^\circ$, it indicates that the sample is hydrophilic, and the smaller the angle, the better the wettability. Good

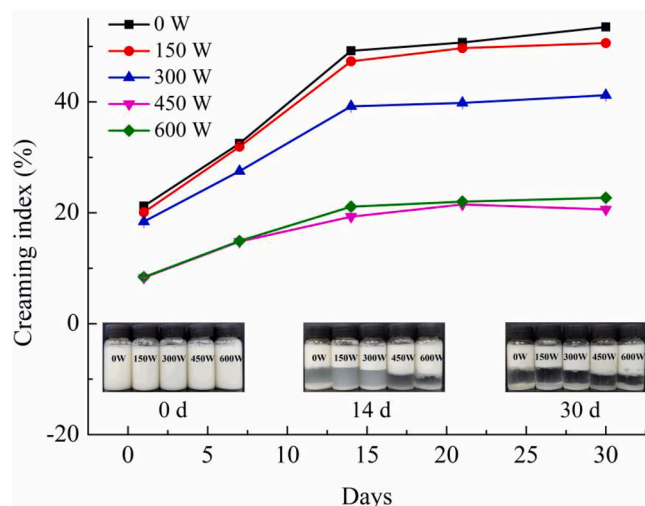


Fig. 8. Storage stability analysis under different ultrasound powers.

wettability favors emulsion processing and absorption in the human body [33]. In Fig. 5A, the θ of all emulsions was $<90^\circ$, which demonstrated that all samples were hydrophilic. Among them, the θ of the emulsion treated at 450 W was the smallest ($29.4 \pm 0.4^\circ$), which was significantly lower than that of the untreated emulsion ($66.2 \pm 0.2^\circ$) ($p < 0.05$). When the HIU power reached 600 W, θ increased again. This may be due to excessive ultrasound treatment resulting in heat and free radicals, which lead to the formation of insoluble aggregates. Furthermore, emulsion stability is closely related to interfacial tension. Decreasing the interfacial tension will enhance the emulsion stability. As shown in Fig. 5B, with increasing HIU power, the particle size of the

emulsion gradually decreased, the interfacial distribution of protein increased, which explained the decrease in interfacial tension. When the emulsion was treated at 450 W, the interfacial tension was the smallest, revealing that the emulsion stability was the best. This agreed with the results of adsorbed proteins and droplet size.

3.7. Apparent viscosity analysis

The association between apparent viscosity and shear rate of the emulsions treated at different HIU powers is shown in Fig. 6. With increasing shear rate, the flow behavior of all emulsions significantly reduced. The untreated emulsion exhibited significant shear thinning behavior and high viscosity. With increasing ultrasound power, the apparent viscosity of the emulsion decreased. Emulsions with smaller particle sizes usually have higher viscosity [34]. The particle size of the emulsion was reduced by ultrasound treatment (Table 1), but the apparent viscosity had the opposite result, probably due to the greater influence of pectin on the emulsion viscosity. This was consistent with the results of Zhang et al. [35]. They found that the molecular weight and apparent viscosity of pectin decreased rapidly after ultrasound treatment.

3.8. Thermal stability analysis

Heat treatment is one of the most commonly used methods in food processing. It can not only exterminate microorganisms but also effectively inactivate protease inhibitors in SPI and improve the nutritive value of SPI. Hence, good thermal stability is essential for emulsion quality. Fig. 7 shows the particle size distribution and appearance changes of the emulsion under different HIU powers after heating. The D_{43} of the untreated emulsion was the largest (2441.07 ± 68.41 nm), implying that the heating treatment caused the emulsion droplets to coalesce and the particle size distribution became uneven [36].

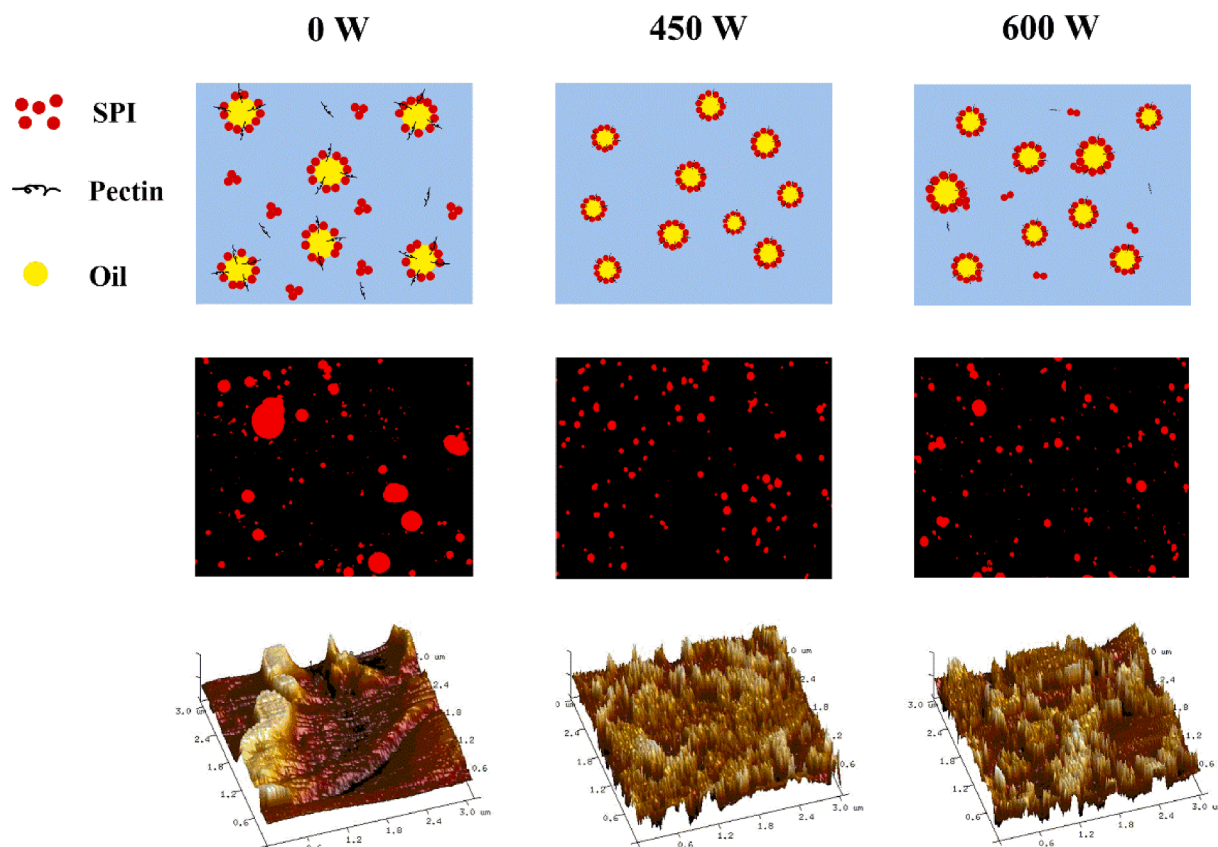


Fig. 9. Mechanism of HIU effect on the SPI-PC emulsion.

Compared with the untreated emulsion, the D_{43} of the HIU-treated emulsion decreased significantly after heating. The D_{43} was minimal (907.95 ± 31.72 nm) when the emulsion was treated at 450 W, and the emulsion separation was also significantly improved. However, the D_{43} increased when the emulsion was treated at 600 W. This may be because the emulsion stability after the 600 W HIU treatment was weaker than that of the 450 W treatment. Concurrently, the heating treatment destroyed the emulsion stability to some extent, causing emulsion droplets to aggregate and D_{43} to increase. The results demonstrated that high HIU power was detrimental to the thermal stability of the emulsion.

3.9. Storage stability analysis

The CI refers to the degree of aggregation and separation of oil droplets from the water phase of the emulsion during storage, which can be used to evaluate the storage stability of emulsion [37]. Fig. 8 shows the CI of the emulsions during storage after HIU treatment at different powers. The freshly prepared emulsion exhibited a uniform milky white color. With prolonged storage time, all the emulsions appeared evidently separated. The CI value of the untreated emulsion during storage was the highest, indicating the worst stability, while HIU treatment can significantly improve this phenomenon. Moreover, the cavitation effect can lead to stronger repulsion between oil droplets, effectively inhibiting coalescence and phase separation of the emulsion [38]. The storage stability of the emulsion was better when the treatment power was higher than 450 W. This was because ultrasound treatment favored the close combination of the complex with the oil droplets, thus promoting emulsion stability.

3.10. Mechanism of the HIU effect on the SPI-PC emulsion

In the HIU emulsification process, three main processes occur: deformation and fracture of the oil droplets, emulsifier transfer and adsorption to the surface of the oil droplets, and emulsified droplets collide with each other and fuse together [39]. The instantaneous rupture of the cavitation bubbles during the HIU process will cause the pressure and volume around the bubbles to change rapidly, resulting in shear force, microjets, and other effects that will affect the emulsion characteristics. The high pressure generated by the bubble rupture will also cause the solid particles and larger droplets suspended in the liquid to be destroyed. In Fig. 9, compared with the untreated emulsion, when the HIU power was 450 W, the particle size of the droplets after the HIU process was significantly reduced and the distribution was more uniform, indicating that the oil droplets were broken and formed small dispersed oil droplets. Concurrently, the SPI-PC complex was subjected to ultrasound treatment, the spatial arrangement changed, and then adsorbed to the surface of the oil droplets quickly to form emulsified droplets. When the HIU power was 600 W, the particle size of the emulsion droplets increased slightly. This might be because the high treatment power caused the local temperature of the sample to increase, and the generated instantaneous high temperature would affect the emulsion performance [40], causing some of the emulsion droplets to collide, aggregate, and fuse.

4. Conclusions

HIU was used successfully to treat emulsions stabilized with SPI-PC complexes. The physicochemical properties, microstructure, and stability of the emulsion were explored. The results demonstrated that HIU treatment significantly enhanced the emulsifying properties of the emulsion. CLSM and AFM images showed that the particle size of the emulsion decreased after treatment, and droplet aggregation was significantly improved. Besides, HIU treatment reduced the interfacial tension and apparent viscosity of the emulsion, and increased its thermal and storage stability. These results demonstrated that HIU can be used in the food industry as a useful technology to enhance emulsion stability.

CRediT authorship contribution statement

Tong Wang: Methodology, Investigation, Writing – original draft. **Ning Wang:** Investigation, Validation, Data curation. **Na Li:** Visualization. **Xiaorui Ji:** Formal analysis. **Hongwei Zhang:** Supervision, Conceptualization. **Dianyu Yu:** Conceptualization, Methodology, Writing – review & editing. **Liqi Wang:** Supervision, Funding acquisition.

Declaration of Competing Interest

The authors declare that they have no known competing financial interests or personal relationships that could have appeared to influence the work reported in this paper.

Acknowledgements

This work was supported by a grant from the National Natural Science Foundation of China (NSFC): Construction of a three-dimensional enzyme electrode and its correlation with phospholipid content in oil (No: 32072259).

References

- [1] S. Park, S. Mun, Y.R. Kim, Emulsifier dependent in vitro digestion and bioaccessibility of beta-carotene loaded in oil-in-water emulsions, *Food Biophys.* 13 (2) (2018) 147–154, <https://doi.org/10.1007/s11483-018-9520-0>.
- [2] J. Liu, H. Zhou, Y. Tan, J. Mundo, D.J. McClements, Comparison of plant-based emulsifier performance in water-in-oil-in-water emulsions: soy protein isolate, pectin and gum arabic, *J. Food Eng.* 307 (3) (2021), 110625, <https://doi.org/10.1016/j.jfoodeng.2021.110625>.
- [3] M.L.F. Freitas, K.M. Albano, V.R.N. Telis, Characterization of biopolymers and soy protein isolate-high-methoxyl pectin complex, *Polímeros* 27 (1) (2017) 62–67, <https://doi.org/10.1590/0104-1428.2404>.
- [4] A. Aguilera-Miguel, E. López-Gonzalez, V. Sadtler, A. Durand, P. Marchal, C. Castel, L. Choplin, Hydrophobically modified dextrans as stabilizers for O/W highly concentrated emulsions. Comparison with commercial non-ionic polymeric stabilizers, *Colloids and Surfaces A: Physicochem. Eng. Aspects* 550 550 (2018) 155–166, <https://doi.org/10.1016/j.colsurfa.2018.04.022>.
- [5] N. Maravić, Z. Šereš, I. Nikolić, P. Dokić, S. Kertész, L. Dokić, Emulsion stabilizing capacity of sugar beet fibers compared to sugar beet pectin and octenyl succinate modified maltodextrin in the production of O/W emulsions: individual and combined impact, *LWT-Food, Sci. Technol.* 108 (2019) 392–399, <https://doi.org/10.1016/j.lwt.2019.03.081>.
- [6] J.I. Horinaka, H. Mori, K. Kani, S. Maeda, Chain mobility of pectin in aqueous solutions studied by the fluorescence depolarization method, *Macromolecules* 37 (26) (2004) 10063–10066, <https://doi.org/10.1021/ma048127m>.
- [7] M. Güzel, Ö. Akpınar, Valorisation of fruit by-products: production characterization of pectins from fruit peels, *Food Bioprod. Process.* 115 (2019) 126–133, <https://doi.org/10.1016/j.fbp.2019.03.009>.
- [8] H. Chen, S. Qiu, J. Gan, Y. Liu, Q. Zhu, L. Yin, New insights into the functionality of protein to the emulsifying properties of sugar beet pectin, *Food Hydrocolloid.* 57 (2016) 262–270, <https://doi.org/10.1016/j.foodhyd.2016.02.005>.
- [9] H. Salminen, J. Weiss, Electrostatic adsorption and stability of whey protein-pectin complexes on emulsion interfaces, *Food Hydrocolloid.* 35 (2014) 410–419, <https://doi.org/10.1016/j.foodhyd.2013.06.020>.
- [10] D.J. McClements, Non-covalent interactions between proteins and polysaccharides, *Biotechnol. Adv.* 24 (6) (2006) 621–625, <https://doi.org/10.1016/j.biotechadv.2006.07.003>.
- [11] A.K. Anal, S. Shrestha, M.B. Sadiq, Biopolymeric-based emulsions and their effects during processing, digestibility and bioaccessibility on bioactive compounds in food systems, *Food Hydrocolloid.* 87 (2018) 691–702, <https://doi.org/10.1016/j.foodhyd.2018.09.008>.
- [12] G. Xu, C. Wang, P. Yao, Stable emulsion produced from casein and soy polysaccharide compacted complex for protection and oral delivery of curcumin, *Food Hydrocolloid.* 71 (2017) 108–117, <https://doi.org/10.1016/j.foodhyd.2017.05.010>.
- [13] A.R. Taherian, M. Britten, H. Sabik, P. Fustier, Ability of whey protein isolate and/or fish gelatin to inhibit physical separation and lipid oxidation in fish oil-in-water beverage emulsion, *Food Hydrocolloid.* 25 (5) (2011) 868–878, <https://doi.org/10.1016/j.foodhyd.2010.08.007>.
- [14] T.S. Perdih, M. Zupanc, M. Dular, Revision of the mechanisms behind oil-water (O/W) emulsion preparation by ultrasound and cavitation, *Ultrason. Sonochem.* 51 (2019) 298–304, <https://doi.org/10.1016/j.ultsonch.2018.10.003>.
- [15] N. Pokhrel, P.K. Vabbina, N. Pala, Sonochemistry: science and engineering, *Ultrason. Sonochem.* 29 (2016) 104–128, <https://doi.org/10.1016/j.ultsonch.2015.07.023>.

- [16] A. Shanmugam, M. Ashokkumar, Functional properties of ultrasonically generated flaxseed oil-dairy emulsions, *Ultrason. Sonochem.* 21 (5) (2014) 1649–1657, <https://doi.org/10.1016/j.ultsonch.2014.03.020>.
- [17] A. Taha, T. Hu, Z. Zhang, A.M. Bakry, I. Khalifa, S. Pan, H. Hu, Effect of different oils and ultrasound emulsification conditions on the physicochemical properties of emulsions stabilized by soy protein isolate, *Ultrason. Sonochem.* 49 (2018) 283–293, <https://doi.org/10.1016/j.ultsonch.2018.08.020>.
- [18] H. Liu, J. Zhang, H. Wang, Q. Chen, B. Kong, High-intensity ultrasound improves the physical stability of myofibrillar protein emulsion at low ionic strength by destroying and suppressing myosin molecular assembly, *Ultrason. Sonochem.* 74 (2021) 105554, <https://doi.org/10.1016/j.ultsonch.2021.105554>.
- [19] C. Li, X. Huang, Q. Peng, Y. Shan, F. Xue, Physicochemical properties of peanut protein isolate-glucomannan conjugates prepared by ultrasonic treatment, *Ultrason. Sonochem.* 21 (5) (2014) 1722–1727, <https://doi.org/10.1016/j.ultsonch.2014.03.018>.
- [20] I.M. Geremias-Andrade, N.P.B.G. Souki, I.C.F. Moraes, S.C. Pinho, Rheological and mechanical characterization of curcumin-loaded emulsion-filled gels produced with whey protein isolate and xanthan gum, *LWT-Food, Sci. Technol.* 86 (2017) 166–173, <https://doi.org/10.1016/j.lwt.2017.07.063>.
- [21] J. Jiang, B. Zhu, Y. Liu, Y.L. Xiong, Interfacial structural role of pH-shifting processed pea protein in the oxidative stability of oil/water emulsions, *J. Agric. Food Chem.* 62 (7) (2014) 1683–1691, <https://doi.org/10.1021/jf405190h>.
- [22] D. Li, Y. Zhao, X.u. Wang, H. Tang, N. Wu, F. Wu, D. Yu, W. Elfalleh, Effects of (+)-catechin on a rice bran protein oil-in-water emulsion: Droplet size, zeta-potential, emulsifying properties, and rheological behavior, *Food Hydrocolloid.* 98 (2020) 105306, <https://doi.org/10.1016/j.foodhyd.2019.105306>.
- [23] N. Wang, X. Zhou, W. Wang, L. Wang, L. Jiang, T. Liu, D. Yu, Effect of high intensity ultrasound on the structure and solubility of soy protein isolate-pectin complex, *Ultrason. Sonochem.* 80 (2021) 105808, <https://doi.org/10.1016/j.ultsonch.2021.105808>.
- [24] T. Wang, K. Chen, X. Zhang, Y. Yu, D. Yu, L. Jiang, L. Wang, Effect of ultrasound on the preparation of soy protein isolate-maltodextrin embedded hemp seed oil microcapsules and the establishment of oxidation kinetics models, *Ultrason. Sonochem.* 77 (2021) 105700, <https://doi.org/10.1016/j.ultsonch.2021.105700>.
- [25] S. Belgheisi, A. Motamedzadegan, J.M. Milani, L. Rashidi, A. Rafe, Impact of ultrasound processing parameters on physical characteristics of lycopene emulsion, *J. Food Sc. Tech. Mys.* 58 (2) (2020) 484–493, <https://doi.org/10.1007/s13197-020-04557-5>.
- [26] T. Wang, X. Chen, W. Wang, L. Wang, L. Jiang, D. Yu, F. Xie, Effect of ultrasound on the properties of rice bran protein and its chlorogenic acid complex, *Ultrason. Sonochem.* 79 (2021) 105758, <https://doi.org/10.1016/j.ultsonch.2021.105758>.
- [27] S. Hu, J. Wu, B. Zhu, M. Du, C. Wu, C. Yu, L. Song, X. Xu, Low oil emulsion gel stabilized by defatted Antarctic krill (*Euphausia superba*) protein using high-intensity ultrasound, *Ultrason. Sonochem.* 70 (2021) 105294, <https://doi.org/10.1016/j.ultsonch.2020.105294>.
- [28] Z. Zhu, W. Zhu, J. Yi, N. Liu, Y. Cao, J. Lu, E.A. Decker, D.J. McClements, Effects of sonication on the physicochemical and functional properties of walnut protein isolate, *Food Res. Int.* 106 (2018) 853–861, <https://doi.org/10.1016/j.foodres.2018.01.060>.
- [29] R. Delahajje, H. Gruppen, M. Giuseppin, P.A. Wierenga, Towards predicting the stability of protein-stabilized emulsions, *Adv. Colloid Interface Sci.* 219 (2015) 1–9, <https://doi.org/10.1016/j.cis.2015.01.008>.
- [30] W. Ma, J. Wang, D.i. Wu, X. Xu, C. Wu, M. Du, Physicochemical properties and oil/water interfacial adsorption behavior of cod proteins as affected by high-pressure homogenization, *Food Hydrocolloid.* 100 (2020) 105429, <https://doi.org/10.1016/j.foodhyd.2019.105429>.
- [31] Y. Li, M. Zhong, F. Xie, Y. Sun, S. Zhang, B. Qi, The Effect of pH on the Stabilization and Digestive Characteristics of Soybean Lipophilic Protein Oil-in-Water Emulsions with Hypromellose, *Food Chem.* 309 (2020) 125579, <https://doi.org/10.1016/j.foodchem.2019.125579>.
- [32] X. Yao, C. Qlab, M. Song, Z. Yi, C. Zbab, C. Lzab, Effect of ultrasound on physicochemical properties of emulsion stabilized by fish myofibrillar protein and xanthan gum, *Innov. Food Sci. Emerg. Technol.* 54 (2019) 225–234, <https://doi.org/10.1016/j.ifset.2019.04.013>.
- [33] L.J. Wang, S.W. Yin, L.Y. Wu, J.R. Qi, J. Guo, X.Q. Yang, Fabrication and characterization of pickering emulsions and oil gels stabilized by highly charged zein/chitosan complex particles (ZCCPs), *Food Chem.* 213 (2016) 462–469, <https://doi.org/10.1016/j.foodchem.2016.06.119>.
- [34] X. Wang, Z. He, M. Zeng, F. Qin, B. Adhikari, J. Chen, Effects of the size and content of protein aggregates on the rheological and structural properties of soy protein isolate emulsion gels induced by CaSO₄, *Food Chem.* 221 (2017) 130–138, <https://doi.org/10.1016/j.foodchem.2016.10.019>.
- [35] L. Zhang, X. Ye, T. Ding, X. Sun, Y. Xu, D. Liu, Ultrasound effects on the degradation kinetics, structure and rheological properties of apple pectin, *Ultrason. Sonochem.* 20 (1) (2013) 222–231, <https://doi.org/10.1016/j.ultsonch.2012.07.021>.
- [36] M. Mehdi, S. Maryam, E.D. Zahra, M. Shima, M. Akbar, Gelation of oil-in-water emulsions stabilized by heat-denatured and nanofibrillated whey proteins through ion bridging or citric acid-mediated cross-linking, *Int. J. Biol. Macromol.* 120 (2018) 2247–2258, <https://doi.org/10.1016/j.ijbiomac.2018.08.085>.
- [37] K.e. Li, Y. Li, C.-L. Liu, L. Fu, Y.-Y. Zhao, Y.-Y. Zhang, Y.-T. Wang, Y.-H. Bai, Improving interfacial properties, structure and oxidative stability by ultrasound application to sodium caseinate prepared pre-emulsified soybean oil, *LWT-Food Sci. Technol.* 131 (2020) 109755, <https://doi.org/10.1016/j.lwt.2020.109755>.
- [38] W. Ma, J. Wang, X. Xu, L. Qin, C. Wu, M. Du, Ultrasound treatment improved the physicochemical characteristics of cod protein and enhanced the stability of oil-in-water emulsion, *Food Res. Int.* 121 (2019) 247–256, <https://doi.org/10.1016/j.foodres.2019.03.024>.
- [39] S. Kentish, T.J. Wooster, M. Ashokkumar, S. Balachandran, R. Mawson, L. Simons, The use of ultrasonics for nanoemulsion preparation, *Innov. Food Sci. Emerg. Technol.* 9 (2) (2008) 170–175, <https://doi.org/10.1016/j.ifset.2007.07.005>.
- [40] L. Zhou, J. Zhang, L. Xing, W. Zhang, Applications and effects of ultrasound assisted emulsification in the production of food emulsions: a review, *Trends Food Sci. Technol.* 110 (2021) 493–512, <https://doi.org/10.1016/j.tifs.2021.02.008>.